applied optics

Wafer-scale arrays of high-Q silica optical microcavities

Erol Ozgur,[1,*] Ersin Huseyinoglu,[1] and Aykutlu Dana[1,2]

[1]UNAM-National Nanotechnology Research Center, Bilkent University, Ankara 06800, Turkey
[2]e-mail: aykutlu@unam.bilkent.edu.tr
*Corresponding author: ozgur@unam.bilkent.edu.tr

Received 20 December 2016; revised 21 February 2017; accepted 21 February 2017; posted 22 February 2017 (Doc. ID 283131); published 16 March 2017

On-chip high-Q microcavities possess significant potential in terms of integration of optical microresonators into functional optoelectronic devices that could be used in various applications, including biosensors, photonic-integrated circuits, or quantum optics experiments. Yet, despite the convenience of fabricating wafer-scale integrated microresonators with moderate Q values using standard microfabrication techniques, surface-tension-induced microcavities (STIMs), which have atomic-level surface roughness enabling the observation of Q values larger than 10^6, could only be produced using individual thermal treatment of every single microresonator within the devised area. Here, we demonstrate a facile method for large-scale fabrication of silica STIMs of various morphologies. Q values exceeding 10^6 are readily obtained using this technique. This study represents a significant advancement toward fabrication of wafer-scale optoelectronic circuitries.

OCIS codes: (220.0220) Optical design and fabrication; (140.4780) Optical resonators; (140.3945) Microcavities.

https://doi.org/10.1364/AO.56.002489

1. INTRODUCTION

Surface-tension-induced microcavities (STIMs) are optical microresonators with substantially diminished surface roughness values, produced by the virtue of thermodynamics compelling materials to have the minimum surface energy possible at their molten states [1]. This type of whispering gallery mode (WGM) microresonators, where light travels in the vicinity of their circumference, have an enhanced capacity for storage of optical power compared with their microfabricated counterparts because optical loss due to surface scattering is thus eliminated [2]. As the figure of merit related to light storage capacity of a microresonator is the quality factor (Q), these microresonators are referred to as possessing high and ultrahigh Q. At the visible and near-infrared wavelengths, silica microresonators could have Q values exceeding 10^9 [1]. The most straightforward method for STIM fabrication is melting the tip of a silica optical fiber using a CO_2 laser [3], while STIM also could be fabricated on-chip by reflowing microdisks [4] in a similar fashion. Diversified applications of STIMs span from optical biosensing [5] to quantum electrodynamics (QED) [6] and also macroscale quantum mechanical observations [7].

While proof-of-principle examples of STIMs have successfully and impressively been demonstrated in well-defined laboratory conditions, their anticipated large-scale applications failed to emerge, coincident with the stagnation in the evolution of their fabrication. One serious and significant bottleneck related to STIMs is their low-throughput fabrication, relying on one-by-one reflow of each microstructure. There are some exceptions such as 2D arrays of chalcogenide microspheres [8] or extremely high-temperature fabrication of wafer-scale all-silica microresonators [9], while affordable wafer-scale production of on-chip STIMs has currently not been demonstrated. Fabrication of STIMs, particularly of silica, in a wafer-scale fashion represents a grave challenge related to materials science.

Here, we demonstrate a novel technique enabling large-scale fabrication of STIMs of various geometries. This facile yet effective method depends on raster scanning of silica microresonators, such as microdisks, to obtain wafer-scale arrays of STIMs, using a CO_2 laser engraver, as schematically demonstrated in Fig. 1. Laser engravers are devices used for laser marking or for cutting predefined shapes out of substrates, which could be plastic, metal, or composite material. The high-energy laser is focused onto the substrate, and either the laser head or the stage is moved to obtain the desired mark or cut shape. This study, to the best of our knowledge, is the first utilization of laser engravers in microresonator fabrication.

2. RESULTS AND DISCUSSION

A. Instrumentation

A CO_2 laser is utilized for reflow of on-chip silica microresonators because the absorption of silica at the wavelength of a CO_2 laser is high, while it is comparably lower in the silicon

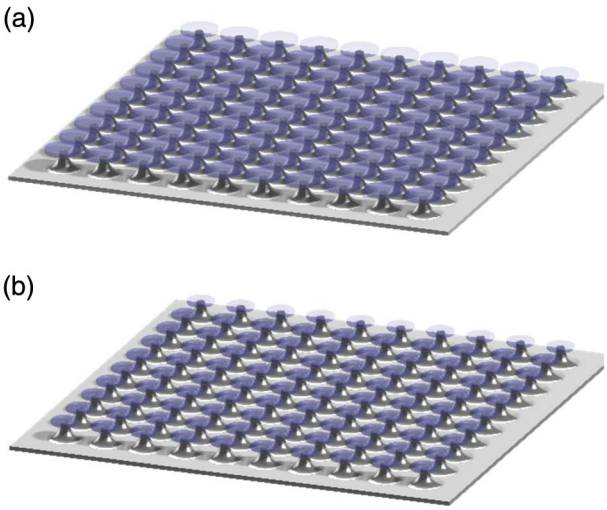

Fig. 1. Array of microdisk (or any arbitrary shape) microresonators produced by microfabrication (a) is completely reflowed to produce high-Q STIMs (b) using raster scanning with a CO_2 laser engraver. This process is suitable to be performed on a wafer scale, once the optimum parameters of focus, laser power, scanning speed, and scanning resolution are determined.

pillar that the resonator stands on. Thus, while the silica part melts after it is exposed to the laser, the silicon pillar acts as a heat sink, controlling the melting process toward formation of a toroidal morphology [10]. Here, the most critical parameter is the temperature of reflow, which depends on the laser power density. Inadequate heating causes partial reflow, while excessive temperatures cause the microresonator to be distorted [11]. The amount of optimum laser energy density is determined mainly by the thickness of the silica layer because the amount of energy absorbed is proportional to the length of the path traveled by the electromagnetic radiation, in accordance with the Beer–Lambert law [12].

For the fabrication of on-chip STIMs, particularly microtoroids, a laser is focused on the microdisk structure, and laser energy is applied. This is performed for each microresonator separately. Therefore, a fabrication process utilizing all advantages of batch production, including photolithography, wet etch, and dry etch, transforms into a tedious task at its final step. Automatization of this step becomes possible using a laser engraver, which would considerably facilitate STIM fabrication. The control over parameters such as focus, laser power, and speed is adequate to obtain desired optical power suitable for reflow of microresonators of various morphologies in a controlled manner.

STIM arrays were microfabricated similar to a previous work [13], except the CO_2 laser reflow. Silicon wafers with 2.5 μm thermal oxide were patterned with photolithography; then the excess silica was removed with buffered HF (BOE) solution. After removal of the photoresist using acetone and isopropanol, the silicon wafer below the silica mask was etched using SF_6 plasma inside an inductively coupled plasma device, forming silica microdisks on silicon pillars, as demonstrated in Fig. 1(a).

Reflow was performed with a CO_2 laser engraver (Zing Laser) using its raster scanning mode. Power was adjusted at 12% (total power = 30 W), while the speed was 2%, corresponding to a scanning speed of 15 mm/s. The resolution was assigned as 1000 DPI to obtain a more uniform reflow. These parameters are not strict because different parameter setting combinations could be applied by altering the focus and power level and reducing the resolution of the scan, which also would affect the amount of interaction of laser and microresonators. The raster scan was done using a rectangular pattern generated in AutoCAD software. The wafer was placed 4 mm out of focus, closer to the laser head, to increase the tunability of optical power, because the power adjustment could only be made in discrete steps.

To observe the optical characteristics of the laser and decipher the effect of performing reflow at out-of-focus configuration, lines were engraved on a Plexiglas substrate by varying the distance according to the focus using the laser engraver. Figure 2 gives the variation of beam diameter with respect

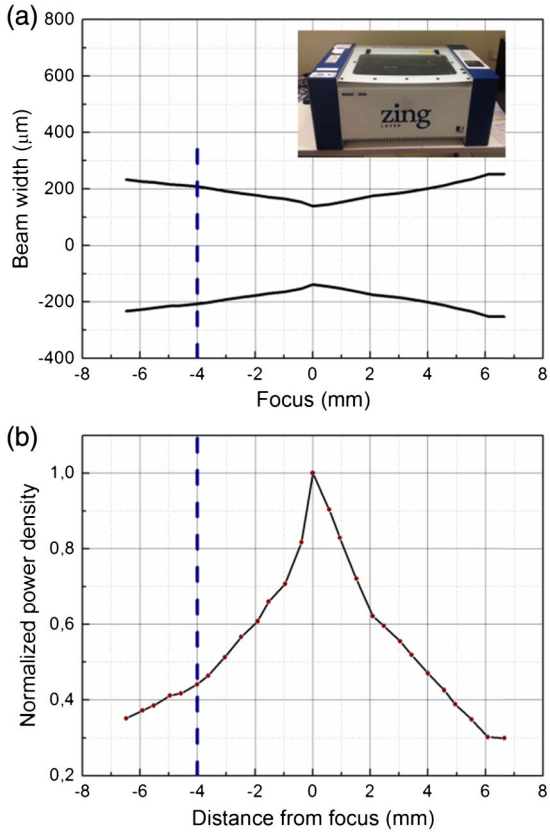

Fig. 2. Investigation of the CO_2 laser beam shape, and the effect of distance on power density for reflow. (a) Lines are engraved onto a Plexiglas substrate by varying the distance from the focus. The line thickness was considered as the beam radius. The beam shape varies with the distance from the focus in a Gaussian shape, as expected. The beam waist and other Gaussian parameters are calculated. The distance of reflow is indicated with the dashed line. The laser engraver is shown in the inset. (b) The graph of power density, decreasing with the inverse of the square of the spot radius. Here, the wafer is placed 4 mm out of focus of the laser, as indicated by the dashed line. Using out-of-focus configuration also enables more precise tuning of the laser optical power because the tuning could be done in discrete steps in the device used in this study.

to the distance from the focus as well as normalized power density, deduced from the relation that the power density is altered with the inverse square of the size of the spot. The beam waist was measured as 140 μm, which corresponds to a Rayleigh range of approximately 6 mm and beam divergence of 24 mrad at 10.6 μm laser wavelength. The beam waist value corresponds to a power density of 58.5 MWm^{-2} at 12% power at focus. When the substrate is 4 mm out of focus, the power density reduces to 26.3 MWm^{-2}, which is still on the same order with the previous reports related to microtoroid fabrication [4]. Here, it could be directly observed that there is an optimum range of reflow, where lower optical power lead to an incomplete reflow, while higher power densities impair the final microtoroid morphology.

B. Characterization

There is significant superiority in using raster scanning instead of individual reflow related to the throughput in the fabrication. Arrays of tens of thousands of STIMs could be produced in parallel within extremely short time spans such as a few hours, provided that the exposure parameters are adjusted. Figure 3 shows SEM images of microresonators produced by this technique. It is virtually impossible to obtain similar results using conventional CO_2 laser reflow. Also, there are no size or planar geometry constraints with this method. Different geometrical shapes of microresonators could be reflowed, independent of their quantity.

Because the most significant figure of merit related to the optical microresonators is the Q value, which represents the ability of a microresonator to store optical energy compared with the loss caused by various factors, including absorption, adsorption, and coupling losses, we measured the Q of the microtoroidal microresonators produced by raster scanning. For this purpose, a rod-shaped wafer (2 mm × 30 mm) containing less dense microdisks was diced before the ICP etch. A less dense configuration was preferred in terms of facilitating fiber-based coupling. The other fabrication steps remained the same. The raster-scanning reflow process was performed using the same parameters, showing the convenience of the suggested approach for sparse array of microcavities. The microtoroids were optically coupled by using a tapered fiber produced by pulling a stripped SMF28 fiber while heating with a hydrogen torch. Light from a tunable external cavity laser (Santec) operating at around 1550 nm was swept within a wavelength range (200 pm) with a sweep rate of 1 nm/s, while the intensity was measured using a powermeter (Newport). The wavelength signal from the laser and the intensity signal from the powermeter were collected by an oscilloscope via a custom-built computer program. The polarization of the laser output was controlled using a fiber polarization controller (Thorlabs) placed after the laser output. The tapered fiber was coupled to the input and output fibers using mechanical couplers.

The resonance dips in the spectrum after the optical coupling were collected and analyzed, and an *ex situ* Lorentzian

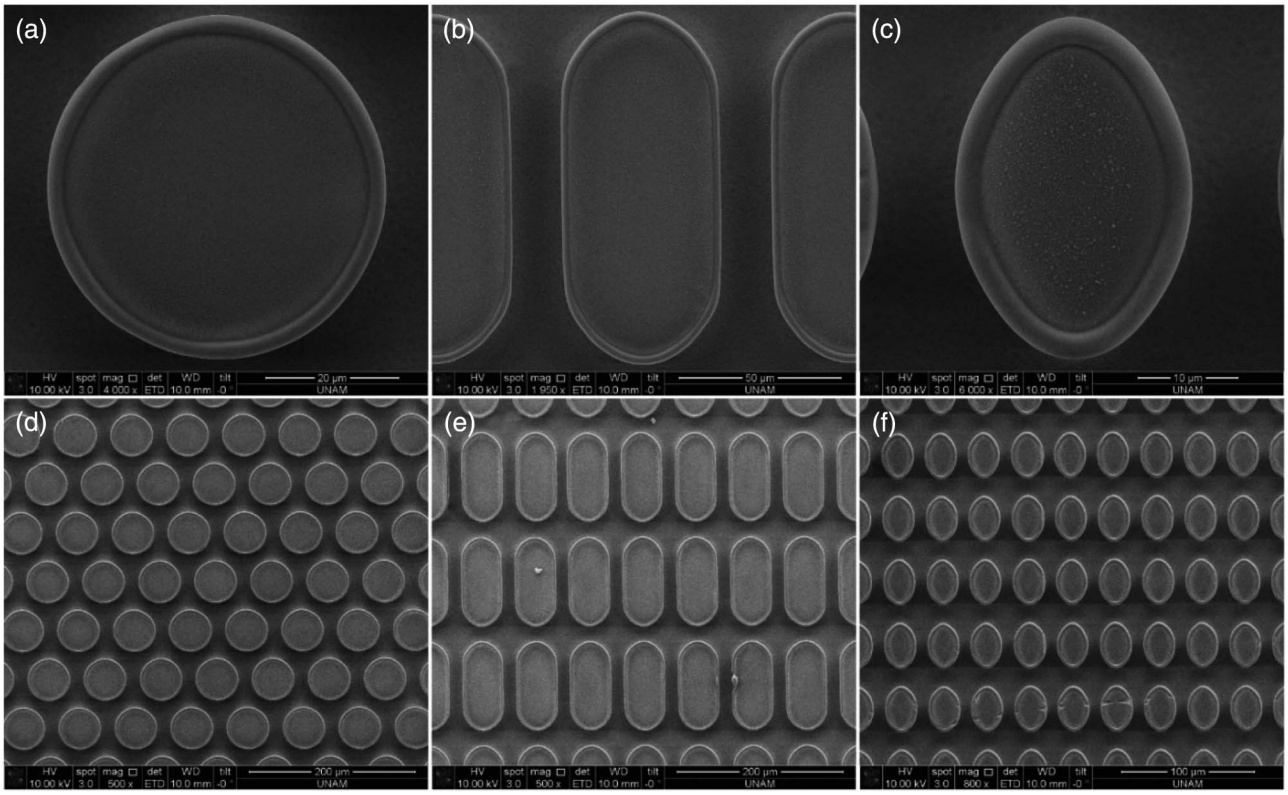

Fig. 3. SEM images of various geometrical shapes of microresonators produced by raster scanning. We demonstrated fabrication of (a), (d) toroidal, (b), (e), racetrack, and (c), (f) elliptical microresonators; yet, other arbitrary shapes are also possible. These microresonators could be produced on a wafer scale via this technique. The density of microresonators also could be arranged depending on the application. Here, a close-pack array is designed.

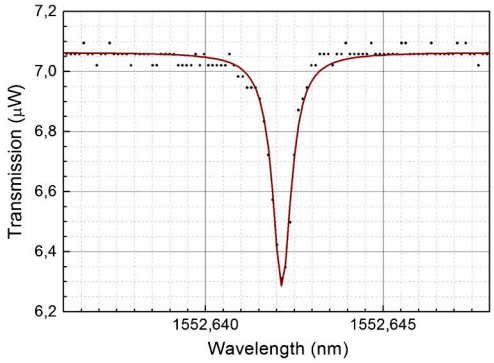

Fig. 4 Resonance dip measured from a microtoroid fabricated using CO_2 laser raster scanning. The Q value is approximately 3×10^6. The data are given with the dots, while the Lorentzian fit is shown with the red line.

fit was performed using a custom-implemented MATLAB script. The resonance dip of a single microtoroid and the Lorentzian fit are given in Fig. 4.

As could be seen in the Fig. 4, the FWHM of the resonance dip is approximately 0.5 pm. From the widely used relation that estimates the quality factor

$$Q = \frac{\lambda}{\Delta\lambda}, \tag{1}$$

the Q value is calculated as approximately 3×10^6, which is relevant to previous reports related to microtoroid fabrication with one-by-one reflow [13]. The diameter of the microtoroid measured was approximately 25 μm.

Wafer-scale arrays of silica STIMs could pave the way for unprecedented large-scale applications of optical microresonators. Large-scale fabrication of on-chip STIM arrays could be readily used for production of giant optoelectronic circuits. Here, the most serious problem is optical coupling to these microstructures. The gap among these microresonators is expected to increase after reflow, due to gathering of material toward the center of each structure. This makes it impossible to obtain optical coupling with a waveguide or another resonator. Yet, this problem could be solved by use of recently proposed alternative fabrication strategies, where reflow is performed to vertical columns instead of horizontal [14]. This is a crucial advantage that mainly could be attained using STIMs. Ultrahigh-Q arrays of microdisks, for instance, produced by careful wet etch [15], are also a similar type of wafer-scale array of on-chip microresonators; yet, they do not possess this intrinsic potential of on-chip coupling because of material loss during wet etch, unless consecutive deposition and patterning steps are applied to fabricate a nearby waveguide, as shown in a very recent work [16]. On the other hand, virtually infinite numbers of optically coupled optoelectronic elements with extremely high light storage and manipulation capacities could be assembled using laser scanning reflow through a relatively more robust course.

Demonstration of fabrication of arbitrary shapes is also important. Nonsymmetrical shapes easily could be used for different purposes such as directional coupling [17] and directional emission [18,19].

One emergent characteristic of raster scanning reflow is that the exposure time, therefore exposure energy of each microresonator, is dramatically small compared with a conventional reflow setup. If there is enough energy, the reflow of silica disks occurs in milliseconds; yet, in conventional systems, because exposing the microtoroid to a CO_2 laser for extended periods does not affect the Q, due to the self-quenching nature of reflow at convenient power levels [4], STIMs are generally subjected to excessive laser illumination. On the other hand, the total energy that each microresonator confronts is approximately 2 orders of magnitude lower in raster scanning. While this is not a fundamental limitation, reflow using laser engraver could thus be considered as more controlled than one-by-one reflow. This outstanding advantage also could be utilized for reflowing different materials that are susceptible to thermal damage or for embedding moderately temperature-resistant functional materials within STIMs, such as silicon nanocrystals [20] and fluorescent nanodiamonds (FNDs) [21] during reflow. Particularly FNDs, which are chemically stable and could withstand temperatures as high as 600°C, could be used to fabricate novel composite optical microresonators in large scales. This characteristic of raster scanning reflow requires further research.

The Q value reported here is 1–2 orders of magnitude lower than most of the other reports related to microtoroidal resonators [4,6]. One significant difference among this report and the mentioned studies is that XeF_2 vapor is used in these studies to etch the silicon underneath silica, while SF_6 plasma is used, due to the unavailability of XeF_2 in our clean room facility, to form the microresonators described here. XeF_2 is extremely selective toward silicon, while the selectivity of SF_6 is relatively low. Thus, the etch process degrades its mask, particularly from the wedges formed during isotropic silica etch with buffered HF. The quality of the final microtoroid morphology, particularly in terms of symmetry, depends mainly on the quality of the microfabrication, i.e., perfect microdisks are required to obtain perfect microresonators [4]. Yet, the Q values obtained in this study could still be considered as high. The time span between the reflow and Q measurement is also critical because it is a well-known fact that water adsorbed on the microresonator surface degrades the Q particularly at infrared wavelengths. The Q values are expected to increase if XeF_2 etch is performed, and Q is measured within a short time after the reflow.

3. CONCLUSION

In conclusion, we demonstrate a significant technical advancement, which could substantially improve the scientific research and applications related to optical microresonators. Hitherto on-chip STIMs could only be fabricated via one-by-one reflow using a CO_2 laser, which was a crucial deficiency, contradicting the nature of batch processing. In this study, we successfully substitute the laser with a laser engraver, providing fabrication of wafer-scale high-Q microresonator arrays. Inherently suitable for all optical integration, this method could lead to various photonic and optoelectronic applications such as multiplexed biosensors with ultimate sensitivity, all optical integrated circuitries, and other on-chip wafer-scale photonic devices.

Also, the extremely controlled nature of this method has potential to enable production of silica-based composite microresonators.

Funding. Türkiye Bilimsel ve Teknolojik Araştırma Kurumu (TUBITAK) (114F481).

Acknowledgment. We thank Caglar Elbuken for the use of the CO_2 laser engraver.

REFERENCES

1. L. Collot, V. Lefevreseguin, M. Brune, J. M. Raimond, and S. Haroche, "Very high-Q whispering-gallery mode resonances observed on fused-silica microspheres," Europhys. Lett. **23**, 327–334 (1993).
2. K. J. Vahala, "Optical microcavities," Nature **424**, 839–846 (2003).
3. D. W. Vernooy, V. S. Ilchenko, H. Mabuchi, E. W. Streed, and H. J. Kimble, "High-Q measurements of fused-silica microspheres in the near infrared," Opt. Lett. **23**, 247–249 (1998).
4. D. K. Armani, T. J. Kippenberg, S. M. Spillane, and K. J. Vahala, "Ultra-high-*Q* toroid microcavity on a chip," Nature **421**, 925–928 (2003).
5. M. D. Baaske, M. R. Foreman, and F. Vollmer, "Single-molecule nucleic acid interactions monitored on a label-free microcavity biosensor platform," Nat. Nanotechnol. **9**, 933–939 (2014).
6. S. M. Spillane, T. J. Kippenberg, K. J. Vahala, K. W. Goh, E. Wilcut, and H. J. Kimble, "Ultrahigh-*Q* toroidal microresonators for cavity quantum electrodynamics," Phys. Rev. A **71**, 013817 (2005).
7. Y. S. Park and H. L. Wang, "Resolved-sideband and cryogenic cooling of an optomechanical resonator," Nat. Phys. **5**, 489–493 (2009).
8. O. Aktas, E. Ozgur, O. Tobail, M. Kanik, E. Huseyinoglu, and M. Bayindir, "A new route for fabricating on-chip chalcogenide microcavity resonator arrays," Adv. Opt. Mater. **2**, 618–625 (2014).
9. K. A. Knapper, K. D. Heylman, E. H. Horak, and R. H. Goldsmith, "Chip-scale fabrication of high-*Q* all-glass toroidal microresonators for single-particle label-free imaging," Adv. Mater. **28**, 2945–2950 (2016).
10. F. Monifi, J. Friedlein, S. K. Ozdemir, and L. Yang, "A robust and tunable add-drop filter using whispering gallery mode microtoroid resonator," J. Lightwave Technol. **30**, 3306–3315 (2012).
11. Y. Yan, S. Yan, G. Jiang, and Z. Ji, "Fabrication of planar microtoroid cavities using high-power laser," Adv. Mater. Res. **60-61**, 347–352 (2009).
12. J. M. Ward, D. G. O'shea, B. J. Shortt, M. J. Morrissey, K. Deasy, and S. G. N. Chormaic, "Heat-and-pull rig for fiber taper fabrication," Rev. Sci. Instrum. **77**, 083105 (2006).
13. E. Ozgur, P. Toren, O. Aktas, E. Huseyinoglu, and M. Bayindir, "Label-free biosensing with high selectivity in complex media using microtoroidal optical resonators," Sci. Rep. **5**, 13173 (2015).
14. X. M. Zhang and A. M. Armani, "Silica microtoroid resonator sensor with monolithically integrated waveguides," Opt. Express **21**, 23592–23603 (2013).
15. H. Lee, T. Chen, J. Li, K. Y. Yang, S. Jeon, O. Painter, and K. J. Vahala, "Chemically etched ultrahigh-Q wedge-resonator on a silicon chip," Nat. Photonics **6**, 369–373 (2012).
16. K. Y. Yang, D. Y. Oh, S. H. Lee, and K. J. Vahala, "Ultra-high-*Q* silica-on-silicon ridge-ring-resonator with an integrated silicon nitride waveguide," in *Conference on Lasers and Electro-Optics (CLEO)* (Optical Society of America, 2016), paper JTh4B.7.
17. C. Li, L. J. Zhou, S. M. Zheng, and A. W. Poon, "Silicon polygonal microdisk resonators," IEEE J. Sel. Topics. Quantum Electron. **12**, 1438–1449 (2006).
18. M. Hentschel, Q. J. Wang, C. L. Yan, F. Capasso, T. Edamura, and H. Kan, "Emission properties of electrically pumped triangular shaped microlasers," Opt. Express **18**, 16437–16442 (2010).
19. X. F. Jiang, Y. F. Xiao, C. L. Zou, L. N. He, C. H. Dong, B. B. Li, Y. Li, F. W. Sun, L. Yang, and Q. H. Gong, "Highly unidirectional emission and ultralow-threshold lasing from on-chip ultrahigh-Q microcavities," Adv. Mater. **24**, 260–265 (2012).
20. A. Tewary, R. D. Kekatpure, and M. L. Brongersma, "Controlling defect and Si nanoparticle luminescence from silicon oxynitride films with CO_2 laser annealing," Appl. Phys. Lett. **88**, 093114 (2006).
21. T. Gaebel, C. Bradac, J. Chen, J. M. Say, L. Brown, P. Hemmer, and J. R. Rabeau, "Size-reduction of nanodiamonds via air oxidation," Diam. Relat. Mater. **21**, 28–32 (2012).